Morphology of Astroglial Cells Is Controlled by Beta-Adrenergic Receptors

W. Shain, D. S. Forman, V. Madelian, and J. N. Turner

Wadsworth Center for Laboratories and Research, New York State Department of Health, Albany, New York 12201; The School of Public Health Sciences, State University of New York at Albany, Albany, New York 12201; Department of Anatomy, Uniformed Services University of the Health Sciences, Bethesda, Maryland 20814-4799

Abstract. Astroglial cells in vivo and in vitro respond to hormones, growth factors, and neurotransmitters by changing from an epithelial-like to stellate morphology. We have studied the temporal relationship between receptor activation, second messenger mobilization, and morphological changes using LRM55 astroglial cells. Maintenance of an altered morphology required continuous beta-adrenergic receptor activation. These changes appeared to be mediated by cAMP since they were elicited by its analogue, dibutyryl cAMP, and by forskolin, a direct activator of adenylate cyclase. Changes in cell morphology may require a relatively small increase in intracellular cAMP, since receptor-stimulated changes in cAMP levels were transient and peaked ~5 min after receptor activation while changes in morphology took at least 30 min to reach a new steady state. Time-lapse videomicroscopy and high voltage electron microscopy indicated that receptor activation resulted in a sequence of morphological events. Time-lapse observations revealed the development and enlargement of openings through the cytoplasm associated with cytoplasmic withdrawal to the perinuclear region and process formation. Higher resolution high voltage electron microscopy indicated that the transition to a stellate morphology was preceded by the appearance of two distinct cytoplasmic domains. One contained an open network of filaments and organelles. The other was characterized by short broad cytoplasmic filaments. The first domain was similar to cytoplasm in control cells while the second was associated with the development and enlargement of openings through the cytoplasm and regions of obvious cytoplasmic withdrawal.

DIFFERENTIATION of astrocytes in vivo (9, 24, 36, 37) and in vitro (8, 13, 14, 16, 21, 25, 32) is associated with dramatic changes in cell morphology. Cells change from an epithelial-like to a stellate morphology. Similar changes are observed in certain populations of astrocytes in the adult brain. Astrocytes in the supraoptic nucleus undergo dramatic morphological changes at parturition and after water deprivation by extending and withdrawing processes (24, 36, 37). When astrocytes in primary cell culture (3, 13–15, 21, 25, 31, 32) or C-6 glioma cells (22) are treated with beta-adrenergic agonists, activators of adenylate cyclase, or analogues of cAMP, cells change from an epithelial-like to a stellate morphology. These studies have demonstrated the occurrence of morphological changes, but have not thoroughly examined the relationships between beta-adrenergic receptor activation, intracellular cAMP, and morphology.

Since activation of beta-adrenergic receptors stimulates the synthesis of cAMP in primary cell cultures of astrocytes (10, 12, 31, 38) and in C-6 cells (6, 23), it has been proposed that changes in morphology result from activation of cAMP-dependent protein kinase (7, 20). Consistent with this hypothesis is the observation that activation of beta-adrenergic receptors results in the phosphorylation of the intermediate filament proteins, glial fibrillary acidic protein (GFAP)[1] and vimentin (7, 20, 25).

LRM55 astroglial cells express a number of phenotypic characteristics common to astrocytes in primary cell culture, including beta-adrenergic receptors that activate adenylate cyclase (18). Furthermore, we have shown that when LRM55 cells are exposed to isoproterenol for periods of time sufficient to produce a change in morphology, i.e., >30 min, there is a transient increase in intracellular cAMP (18). In this report we present data describing the temporal relationship between receptor occupancy, intracellular cAMP accumulation, and changes in cytoarchitecture associated with changes in cell morphology.

Materials and Methods

Cells and Growth Conditions

Cells were grown in modified Ham's F-12 medium (18) supplemented with 5% FBS. For quantitative light microscopic analysis, 1-3 × 10^4 cells in a

1. *Abbreviations used in this paper*: GFAP, glial fibrillary acidic protein; HBHS, Hepes-buffered Hanks' saline.

400-μl aliquot were plated on 11 × 22-mm glass coverslips in 35-mm culture dishes. Coverslips were sterilized by cleaning in 70% ethanol and flaming. Surface tension kept the aliquot isolated on the coverslip, and the following morning, after cells had attached, the dish was flooded with 2 ml of growth medium. Cells were allowed to grow until they were ~50% confluent. For time-lapse video microscopy, cells were plated onto 24.5-mm round coverslips (Nicholson Precision Instruments, Gaithersburg, MD) using a similar procedure. For ultrastructural analysis cells were plated onto Formvar-carbon-coated gold grids secured to a coverslip by Formvar-carbon film. The coverslips, films, and grids were sterilized in 35-mm culture dishes by ultraviolet irradiation.

Cells were washed free of growth medium by rinsing three times with Hepes-buffered Hanks' saline (HBHS) (30) at 37°C before exposure to receptor agonists and preparation for cAMP analysis or fixation.

Time-Lapse Videomicroscopy

Coverslips were transferred to a Dvorak-Stotler chamber (11) (Nicholson Precision Instruments, Rockville, MD) in culture medium. After mounting in the chamber, cells were continuously perfused with HBHS at 0.4 ml/h using a syringe pump (model 341; Sage Instruments, Cambridge, MA). Faster perfusion (0.9 ml/min) was used for rapid addition of (−)-isoproterenol or control (HBHS) solutions. Cells were observed with an upright Zeiss microscope using a 40× planachromatic objective and Nomarski differential interference contrast optics. Video-enhanced contrast was obtained using a Hamamatsu C1000-01 video camera (1). Images were recorded in time-lapse mode using a Panasonic NV-8050 video cassette recorder, so that time was speeded up by a factor of six. The final magnification on the video monitor was 3,200. The light path included a Calflex heat reflection filter and monochromatic green filter (Zeiss VG9; 546 nm). The chamber was maintained at 35°C using an Air Stream Stage Incubator (model C300; Nicholson Precision Instruments), and temperature was monitored using a thermistor taped to the Dvorak-Stotler chamber.

cAMP Measurement

The intracellular cAMP content was measured by an HPLC separation method (19) adapted from the procedures of Lin et al. (17). Briefly, cells were grown in 24-well trays and incubated at 37°C with 250 μl of [^{3}H]adenine in HBHS (10 μCi/ml) for 60 min to label the intracellular ATP pool. cAMP production was stimulated by adding 25 μl of agonist. After further incubation, the reaction was stopped by aspirating the medium, and adding 250 μl 0.3 M NaOH. 10 μl of cold cAMP (0.1 mg/ml) was added to each sample as a marker. The contents of the wells were transferred to a microcentrifuge tube, the wells were washed with 250 μl of H_2O, and the wash added to the same tube. Proteins and noncyclic nucleotides were precipitated by adding 100 μl $ZnSO_4$ (0.75 M) and separated from the cAMP-containing supernatant by centrifugation. A 50-μl portion of the cell supernatants was injected into a 5-mm NOVA-PAK C18 Radial-PAK cartridge (Waters Associates, Milford, MA).

cAMP was separated from other radiolabeled adenine derivatives using a mobile phase of 0.1 M $(NH_4)_2PO_4$, 1% methanol, pH 3.0, pumped at 1 ml/min. The eluate fractions containing the cAMP were collected and radioactivity was measured by liquid scintillation counting. Recovery of cAMP using this method was >90% and variation between triplicate wells was <10%.

Protein content of cell samples was measured by a dye-binding method (3).

Preparation of Cells for Quantitative Morphologic Analysis

After experimental treatments, cells were fixed for 10 min in 2% glutaraldehyde in s-collidine buffer, pH 7.4, at 37°C, rinsed in HBHS, rinsed rapidly in distilled water, and mounted directly onto slides with a waterbased mounting medium (Glycergel; Dako Corp., Santa Barbara, CA). Cells were observed and photographed using phase contrast or differential interference contrast optics with a Leitz Ortholux 2 microscope.

Quantitative analysis was done using coded slides to prevent the scorer from knowing the treatment of samples being observed. Changes in cell morphology were measured by observing randomly chosen fields on each coverslip. All cells within each field were scored, and 10 fields or at least 250 cells were observed on each coverslip. Transition to a stellate morphology was defined as the formation of spikelike processes. Cells were scored as "plus" or "minus" bearing spikes. Any cell with at least one process as long as the long axis of the perinuclear region was scored "plus". These cell counts were then used to calculate the percentage of cells bearing spikes ([cells bearing spikes/total cells observed] × 100).

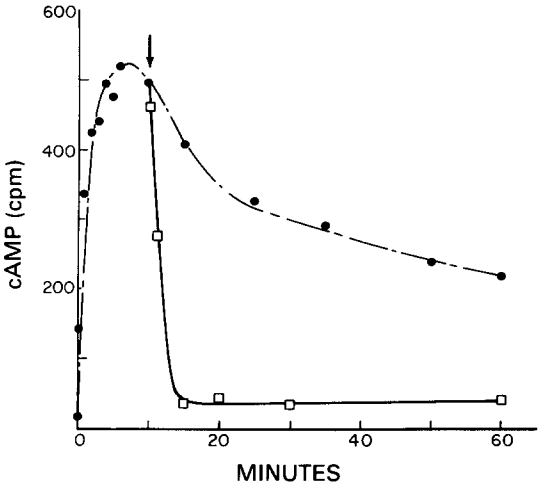

Figure 1. Time course of cAMP accumulation in LRM55 astroglial cells after stimulation with the beta-adrenergic agonist (−)-isoproterenol (*solid circles*) and inhibition by the beta-adrenergic antagonist propranolol (*open squares*). All cells were continuously exposed to 100 nM (−)-isoproterenol. After 10 min (*arrow*) one set of cells was additionally treated with 100 μM propranolol.

Preparation of Cells for High Voltage Electron Microscopy (HVEM)

Cells were treated and fixed in glutaraldehyde as described above, postfixed in 1% s-collidine-buffered OsO_4 at room temperature for 10 min, stained en bloc using 2% aqueous uranyl acetate for 20 min, dehydrated in graded ethanols, and critical point dried from CO_2. Three 100% ethanol dehydration steps were used, the last two with ethanol stored over a molecular sieve for at least 2 mo to remove residual water. Two other precautions were also taken to eliminate H_2O during critical point drying. Grade IV CO_2 was used with ~10 ppm residual H_2O and the gas was passed through an in-line molecular sieve between the tank and critical point drying unit. During CO_2 exchanges the critical point drying unit was agitated to insure complete flushing of the ethanol (28).

Cells were observed at 1.0 MeV in the Wadsworth Center for Laboratories and Research AEI Mark VII 1.2 MeV HVEM using the stage and methods previously described (33–35).

Results

Activation of beta-adrenergic receptors on LRM55 astroglial cells with 100 nM (−)-isoproterenol resulted in a rapid increase in the intracellular concentration of cAMP (Fig. 1). Intracellular cAMP levels reached a maximum ~5 min after receptor activation and then declined to <50% of the maximum after 60 min. The elevated levels of intracellular cAMP were the result of continuous receptor activation since inhibition of receptor activation of adenylate cyclase by subsequent addition of 100 μM propranolol, a beta-adrenergic antagonist, caused a rapid drop in the intracellular cAMP levels to control values (Fig. 1, *open squares*).

The effects of beta-adrenergic receptor stimulation on cell morphology were observed both by continuously viewing cells using time-lapse videomicroscopy (Fig. 2) and by fixing cultures at various times after exposure and determining the percentage of cells bearing spikes (Fig. 3). When cells were perfused with 1 μM (−)-isoproterenol, a concentration suf-

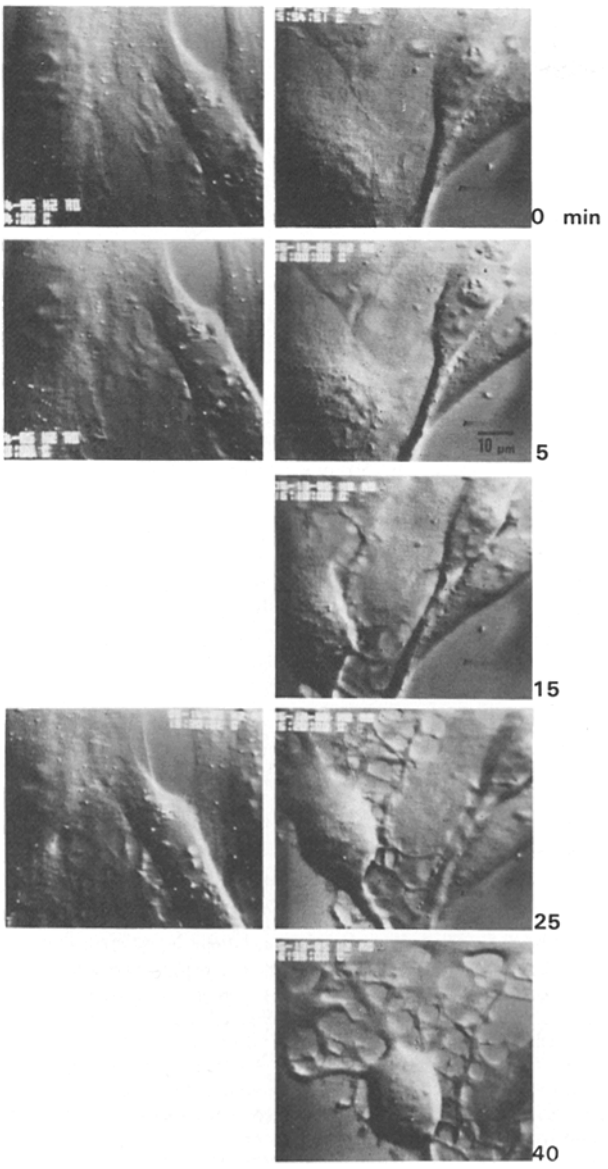

Figure 2. Time-lapse videomicroscopy of (−)-isoproterenol-stimulated changes in cell morphology. Control cells (*left*) were continuously perfused with HBHS. Treated cells (*right*) were continuously perfused with 1 μM (−)-isoproterenol. These images were obtained at the times indicated at the lower right corners of the micrographs.

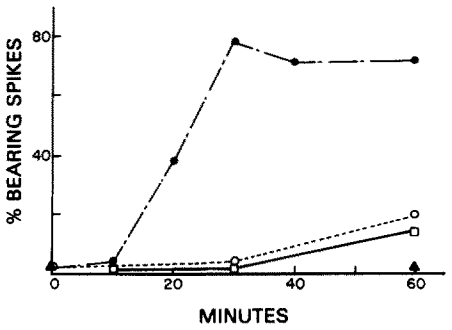

Figure 3. Quantitative analysis of the time course of (−)-isoproterenol-stimulated change in cell morphology. Cells were treated with 100 nM (−)-isoproterenol (*solid circles*), 100 nM (+)-isoproterenol (*open circles*), 100 nM (−)-isoproterenol, and then additionally with 100 μM propranolol after 10 min (*open squares*), or with HBHS (*solid triangles*). Changes in morphology were quantitated by determining the percent of cells bearing spikes.

ficient to maximally activate cAMP production (18), subtle changes in cell morphology were observed almost immediately by time-lapse videomicroscopy. The first effects of the beta agonist were observed as an apparent increase in saltatory movement of cell organelles; subsequently cytoplasm withdrew toward the perinuclear region, which became thicker and more rounded (see micrograph at 5 min, Fig. 2). Cytoplasmic withdrawal and process formation was associated with the development of openings through the cytoplasm. We will call these openings "embrasures". Embrasures developed as a result of slow withdrawal of cytoplasm. Processes formed as numerous embrasures enlarged (see micrographs at 15, 25, and 40 min, Fig. 2). As this process of embrasure opening and enlargement continued, one or several major processes developed with many shorter secondary processes (see 25-min micrograph, Fig. 2). Smaller processes continued to form for as long as cells were observed (60 min). No membrane ruffling was associated with the withdrawing plasma membrane. No changes in morphology were observed in control cultures (see Fig. 2, left).

The change in cell morphology was quantified as a percentage of cells bearing spikes at various times after treatment (see Materials and Methods). Using the criteria of at least one process equal in length to the diameter of the perinuclear region for measuring changes in cell morphology, we did not observe any significant changes until after 10 min of treatment (Fig. 3). By 30 min, the number of cells bearing processes had reached a maximum and remained constant for an additional 30 min. In other experiments we have observed that spikelike projections are maintained after 24 h of continuous treatment with (−)-isoproterenol (100 nM–1.0 μM).

Two experiments demonstrate that the effects of (−)-isoproterenol occurred via specific interaction with beta adrenergic receptors. First, cells were treated with the optically inactive isomer (+)-isoproterenol (Fig. 3, *open circles*). (The beta-adrenergic receptor has high stereo selectivity for agonists; (+)-isoproterenol is ~100-fold less effective than the stereoactive isomer for stimulating cAMP synthesis [18]). When cells were treated with 100 nM (+)-isoproterenol no change in morphology was observed at 30 min and by 60 min <20% of the cells had changed shape. These changes may be due to the weak agonist activity of this isomer.

In a second experiment cells were first incubated with 100 nM (−)-isoproterenol for 10 min and then continuously exposed to (−)-isoproterenol and 100 μM propranolol for a total of 60 min (Fig. 3, *open squares*). These conditions should have produced a rapid fall in the intracellular cAMP levels after the maximum level had been reached (see Fig. 1). No changes in cell morphology were observed at 30 min and only a few cells had changed shape by 60 min. No changes in cell morphology were observed in control cells (Fig. 3) after 60 min incubation in HBHS. Thus, (−)-isoproterenol-stimulated changes in cell morphology are the result of specific activation of beta-adrenergic receptors and continu-

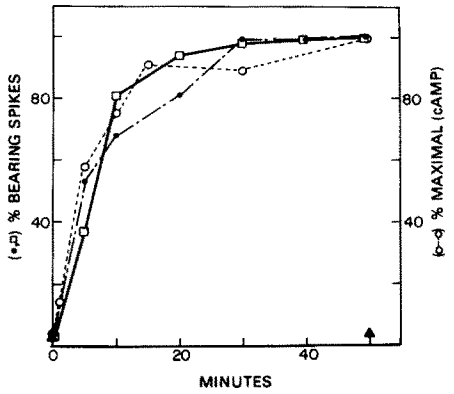

Figure 4. Time course of changes in cell morphology after stimulation with dibutyryl cAMP (*open squares*) and forskolin (*solid circles*) and increases in intracellular cAMP after stimulation with forskolin (*open circles*). Cells were continuously exposed to either 1 mM dibutyryl cAMP or 10 μM forskolin and either fixed for quantitation of changes in morphology or prepared for cAMP analysis.

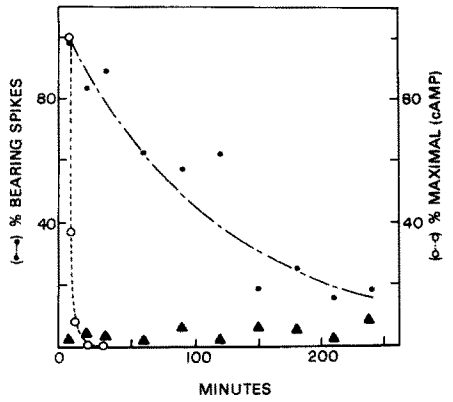

Figure 6. Time courses of the effects of removing (−)-isoproterenol from LRM55 cells. For quantitation of changes in cell morphology, cultures were treated with either (−)-isoproterenol (*solid circles*) or HBHS (*solid triangles*) for 30 min, washed three times with HBHS, and incubated for the indicated times in HBHS. For analysis of intracellular cAMP, cells were treated for 5 min, a time sufficient to obtain a maximal response to (−)-isoproterenol, washed three times with HBHS, and incubated for the indicated times in HBHS (*open circles*).

ous receptor activation is required for changes in cell morphology to occur.

Dibutyryl cAMP and forskolin were used to demonstrate that observed changes in cell shape were due to receptor-activated increases in intracellular cAMP. Dibutyryl cAMP is a membrane-permeable analogue of cAMP and caused rapid changes in LRM55 astroglial cell morphology similar to those observed with (−)-isoproterenol (Fig. 4, *open squares*). Forskolin is a direct activator of adenylate cyclase (2, 29). When cells were treated with 10 μM forskolin, parallel increases in intracellular cAMP (Figure 4, *open circles*) and cells bearing spikes (*solid circles*) were observed. The effects of dibutyryl cAMP and forskolin reached a maximum by 20 min and were maintained for 60 min.

In all experiments observing shape change some cells (≤25%) did not develop processes, but became very flat and thin. These cells may represent a subset of cells within the population that cannot form embrasures and processes or may be proceeding to change shape at a slower rate.

If maintenance of the process-bearing morphology requires continuous receptor activation the effects of the receptor agonist should be reversible. To test this hypothesis, cells were treated with 100 nM (−)-isoproterenol for 60 min, washed free of (−)-isoproterenol by removing the incubation medium, rinsed three times with HBHS, incubated with HBHS for additional times, fixed, and observed. Cells slowly returned to their control morphology ($t_{1/2}$ = 90 min) (Figs. 5 and 6, *solid circles*). This process was much slower than the observed decrease in intracellular cAMP after washing cells free of (−)-isoproterenol ($t_{1/2}$ ≤2 min) (Fig. 6, *open circles*). Nonstimulated controls showed no change in morphology (Fig. 6, *solid triangles*). It appeared that the return to a morphology similar to that observed before treatment occurred by the moving of cytoplasm back down the spikelike processes (Fig. 5).

Higher resolution studies of cell morphology were carried out on whole mounts prepared for HVEM. In control cells (Fig. 7 *A*) the thinner peripheral cytoplasm was uniform, extensively spread, and contained filamentous elements. The number of mitochondria decreased as the cytoplasm thinned and delicate vertical filopodia and microspikes were occa-

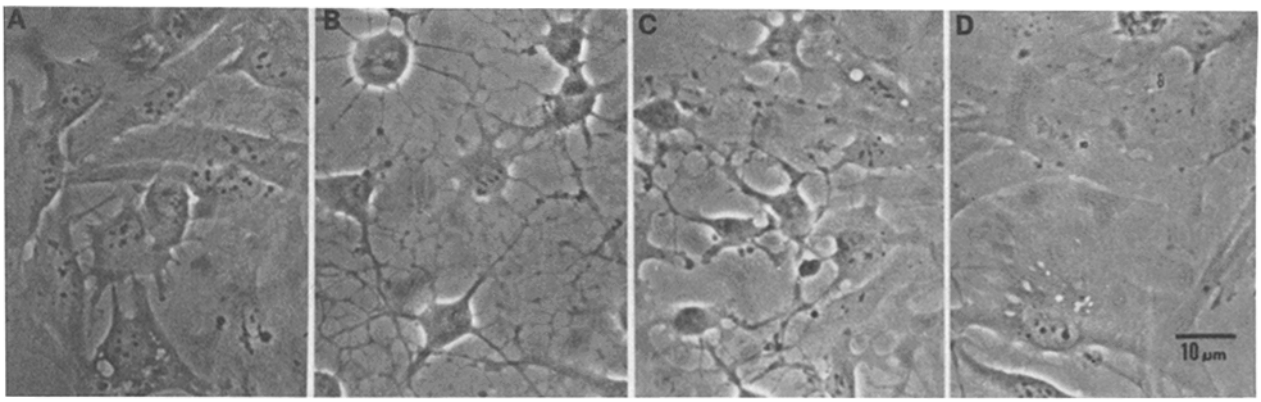

Figure 5. Phase-contrast micrographs illustrating representative fields of fixed LRM55 cells used for the quantitative analysis presented in Fig. 6. Cells were treated for 30 min with HBHS (controls) (*A*) or 100 nM (−)-isoproterenol for 30 min and washed three times with HBHS and then further incubated for 0 min (*B*), 90 min (*C*), or 180 min (*D*).

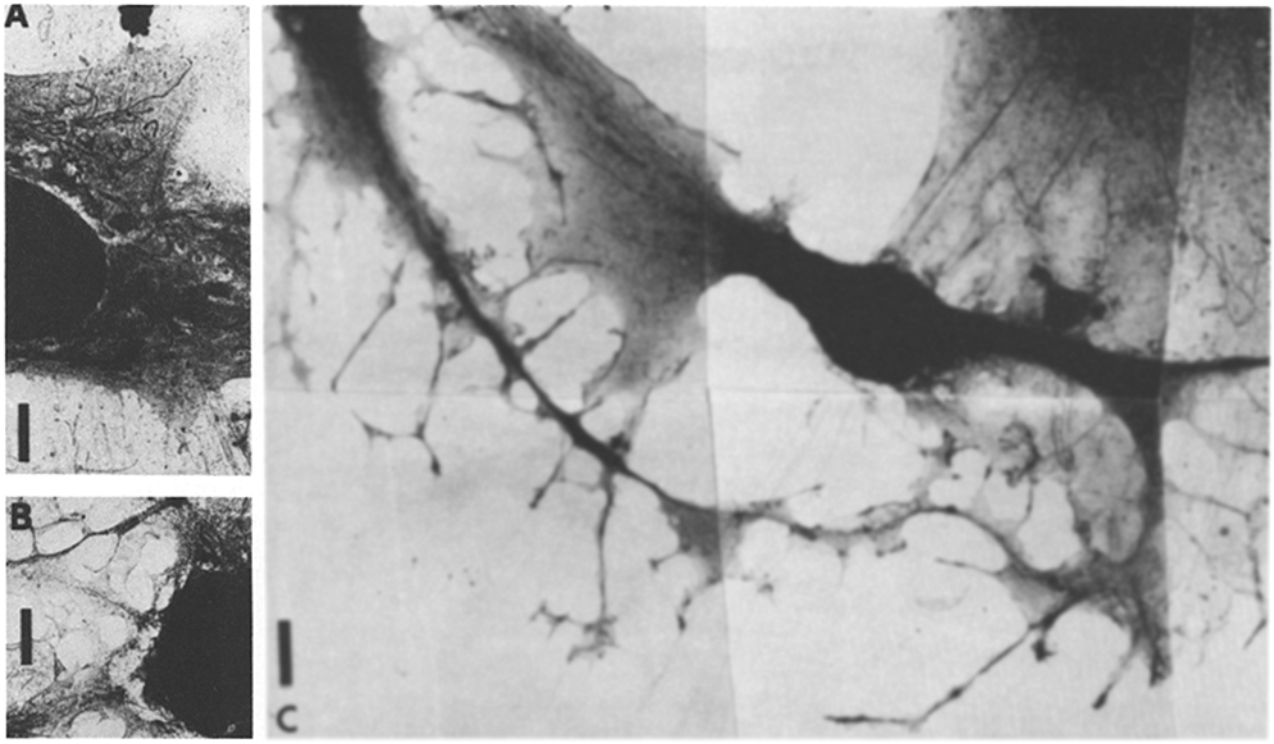

Figure 7. HVEM micrographs of control and treated cells demonstrating morphologic changes. (*A*) Control cells with spread cytoplasm and easily penetrated nucleus. (*B*) Cells treated with 100 nM (−)-isoproterenol for 20 min show radially distributed embrasures and a nuclear region impenetrable to the electron beam. (*C*) A montage of portions of three treated cells. The cell bodies and areas of the large processes were not penetrated. Two of the cells show dramatic changes in cell morphology with long narrow primary processes and many smaller projections resulting in a scalloped appearance. The Formvar-carbon substrate has been wrinkled by the cell in the center. The non–process-bearing cell at upper right also has a thickened perinuclear region indicating cytoplasmic withdrawal. Bars, 10 μm.

sionally observed. The perinuclear region was relatively thicker but readily penetrated by the 1.0-MeV electron beam.

The peripheral regions of cells fixed after 20 min treatment with (−)-isoproterenol were generally thinner and contained fewer organelles than controls. The periphery of some cells contained large numbers of embrasures (Fig. 7 *B*) and the organelles appeared not to be uniformly distributed (Fig. 7 *C*, upper right). Major processes were apparent in cells in which embrasures were more numerous and had enlarged (Fig. 7 *C*, center and lower right). The increase in electron density of the nuclear regions and primary processes was coupled with embrasure development indicating the withdrawal of cytoplasm from the periphery into these regions. Video light microscopy indicated that active cytoplasmic movement and withdrawal occurred at these sites. Most cells had one or two major processes corresponding to the primary axis and numerous smaller processes producing a scalloped appearance along the cell periphery. The carbon-coated Formvar substrate was usually observed to be wrinkled under the perinuclear region of cells with well-developed processes. The wrinkles were perpendicular to the primary axis of the cell, indicating that the withdrawal of cytoplasmic elements to the perinuclear region occurred by means of active contraction (see Fig. 7 *C*).

In broad peripheral regions, the cytoplasm appeared to be organized into organelle-free and organelle-containing domains (Figs. 7 and 8). In many cells these domains were radially organized and parallel (Fig. 8). The cytoplasm in organelle-containing domains consisted of an open network of delicate uniform filaments. The cytoplasm of the organelle-free domains consisted of a denser network that appeared fused and condensed (see regions *F* and *C*, respectively, in Figs. 8 and 9). Regions of condensed cytoplasm were usually associated with embrasure development and enlargement, including the finer processes producing the scalloped appearance of the cell periphery (Figs. 7 *C* and 9). These regions were not exclusively observed along the periphery of cells, but were also seen in more central portions of cytoplasm (Figs. 7 *B*). Treated cells commonly exhibited condensed cytoplasm, and the transition from filamentous to condensed was abrupt (Figs. 8 and 9). Similar condensation was rarely observed in control cells, and then only in regions exhibiting vertical projections and filipodia indicative of cytoplasmic motion.

Discussion

Activation of beta-adrenergic receptors on LRM55 astroglial cells results in a cAMP-dependent change in cell morphology similar to that observed in astrocytes in primary cell culture (8, 14, 21, 25) and C-6 astrocytoma cells (22). In this study we have described the initial changes that occur in intracellular cAMP and cell morphology after receptor stimulation. Intracellular cAMP levels rise rapidly, reach a peak after 5 min, and decay towards control levels. However, changes in cell morphology have a different time course.

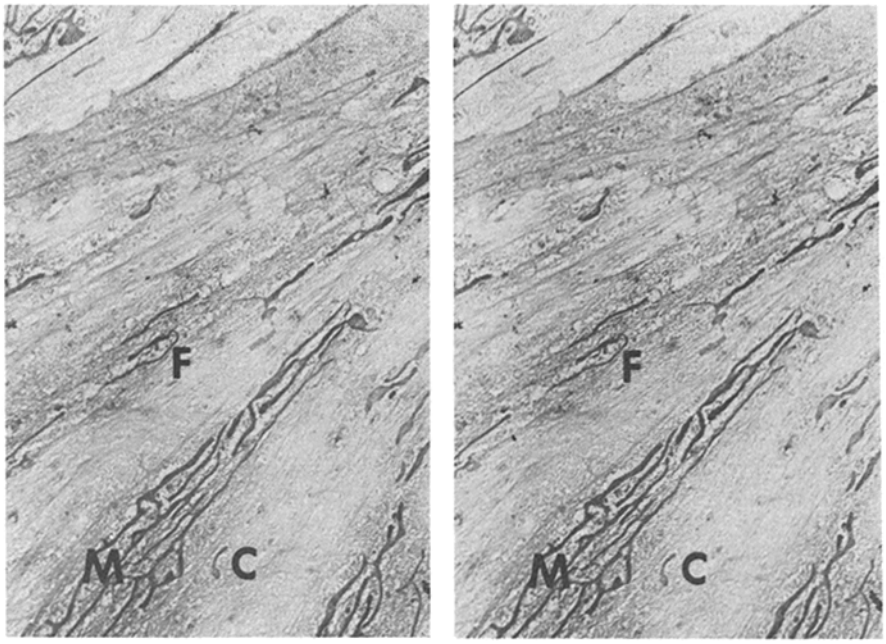

Figure 8. A stereopair of HVEM micrographs showing a portion of a cell treated with 100 nM (−)-isoproterenol for 20 min. The cytoplasm is divided into organelle-containing and organelle-free regions that are parallel to the filamentous cytoskeletal components. The cytoplasm is of three types: long filamentous in the regions of mitochondria (*M*) and either short filamentous (*F*) or condensed (*C*) in organelle-free regions. Bar, 2 μm.

While some changes are observed almost immediately, the most obvious do not begin for 5–10 min and continue for at least 30 min before an apparent steady-state condition is observed. Two observations indicate that changes in cell morphology require continuous beta-adrenergic receptor activation. (*a*) If after an initial 10-min period of activation further receptor function is blocked by addition of the beta-adrenergic antagonist propranolol, cells fail to change shape (Fig. 3). (*b*) Removal of the receptor agonist after cells have changed shape results in a return of cells to preexposure morphology (Figs. 5 and 6).

Activation of beta adrenergic receptors results in activation of adenylate cyclase and increases in intracellular cAMP (18). Two additional observations are consistent with the hypothesis that shape change results from increases in intracellular cAMP. First, treatment of cells with the cAMP analogue dibutyryl cAMP resulted in changes in cell morphology (Fig. 4). Second, forskolin, a direct activator of adenylate cyclase (2, 29), produced changes in intracellular cAMP and cell morphology similar to those observed with the beta-adrenergic agonist (Fig. 4). Thus, the pharmacological data indicate that beta-adrenergic receptor-mediated changes, in cell morphology are cAMP-dependent and require continuous receptor activation.

Since cAMP functions in cells to activate cAMP-dependent protein kinase, beta-adrenergic-stimulated changes in cell morphology may result from phosphorylation of cellular proteins. Consistent with this hypothesis is the observation

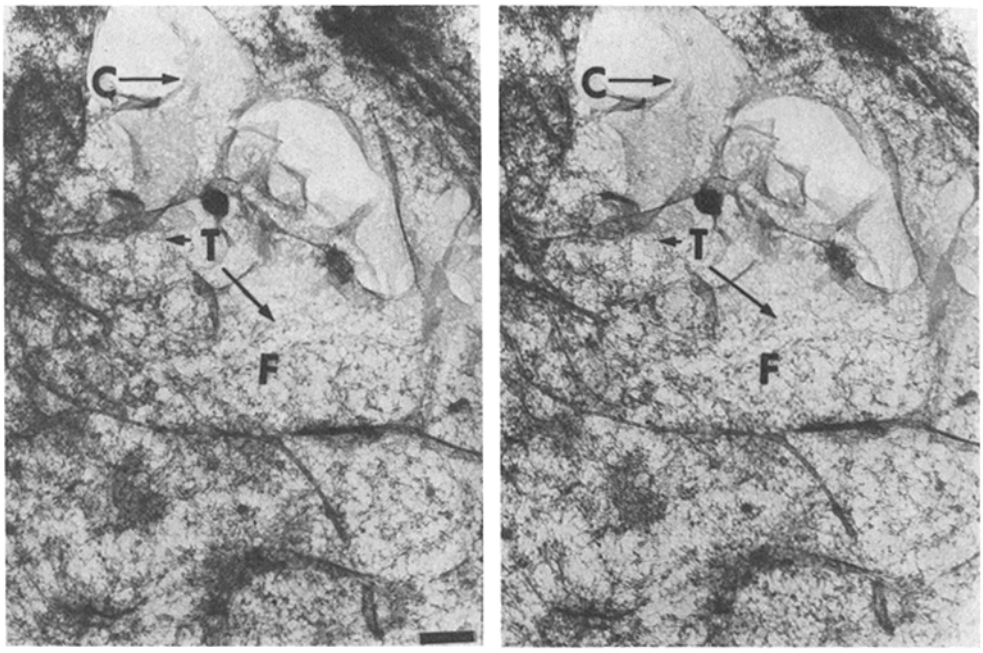

Figure 9. A stereopair of HVEM micrographs illustrating an area of embrasure formation near the perinuclear region of a cell treated with 100 nM (−)-isoproterenol for 20 min. Condensed (*C*) and filamentous (*F*) regions of cytoplasm are seen as well as a transition zone (*T*). The edges of the embrasure contain numerous thin vertical lamellae. The dark region above the *T* is a surface projection. Bar, 1 μm.

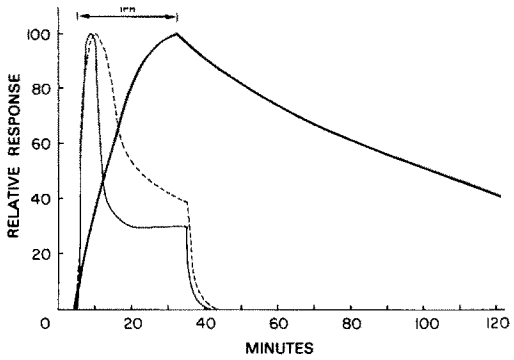

Figure 10. Comparison of time-dependent changes in intracellular cAMP (*broken line*), taurine release (*solid line*), and cell morphology (*bold line*) after beta adrenergic receptor activation in LRM55 astroglial cells. This figure has been developed from representative data presented in this report as well as a previously published description of intracellular cAMP accumulation and taurine release (18).

that several cytoskeletal proteins (GFAP and vimentin) are phosphorylated by cAMP-dependent protein kinase and a Ca^{++}-sensitive, phosphoinositol-dependent protein kinase (7, 20, 25). Treatment of primary cultures of astrocytes with phorbol esters, activators of Ca^{++}-sensitive, phosphoinositol-dependent protein kinase, produces changes in cell morphology. Thus, morphologic changes may be regulated by several different intracellular pathways acting on common cellular constituents. Vimentin and GFAP, however, may not be these constituents since Pollenz and McCarthy (25) have demonstrated temperature-dependent changes in cell morphology without phosphorylation of these proteins. Thus, the relationship between phosphorylation of GFAP and vimentin and changes in cell morphology is not clear.

While changes in cell morphology may result from increases in intracellular cAMP levels, cAMP-dependent protein kinase activation, and protein phosphorylation, the mechanisms by which these processes regulate cell function are not clear. Our previous data (18, 31) and that of others (10, 23) indicates that activation of adenylate cyclase produces significantly greater amounts of cAMP than those required to maximally activate cellular responses. For instance, activation of beta adrenergic receptors on LRM55 astroglial cells and primary cultures of astrocytes stimulates release of taurine. Maximal taurine release is stimulated by a concentration of (−)-isoproterenol that produces a small increase in intracellular cAMP, ~10% of a maximal response (18, 31). Comparison of the time courses for receptor-stimulated increase (Fig. 10) in intracellular cAMP levels (*broken line*), taurine release (*solid line*), and changes in cell morphology (*bold line*) indicate that taurine release and cell morphology are regulated differently. During continuous receptor stimulation taurine release peaks rapidly, reaches an elevated steady-state, and after removal of the agonist, abruptly returns to baseline ($t_{1/2} \leqslant 3$ min) (18, 31). Changes in morphology begin more slowly, reaching an apparent maximum only after ~30 min. This new morphology is maintained for as long as the agonist is present. Cells slowly return to the control morphology when the agonist is removed ($t_{1/2} = 90$ min). These observations indicate that activation of the same second messenger pathway may result in differential regulation of distinct cellular processes.

HVEM of control and (−)-isoproterenol-treated cells have made it possible to study changes in cytoarchitecture after receptor stimulation. The transition to a stellate morphology appears to follow a definite course. First, a redistribution of intracellular organelles occurs, followed by the development of embrasures that increase in number and size until processes develop and cytoplasm is withdrawn to the perinuclear region (Figs. 2, 7 *B*, 8, and 9). A number of observations are consistent with this hypothesis. First, time-lapse videomicroscopy indicates an increase in saltatory organelle movement and the dynamic development of embrasures. Second, HVEM observations showed that embrasures develop in organelle-free regions. Third, embrasures develop and enlarge adjacent to regions that become processes. Fourth, light and electron microscopic observations indicate that the perinuclear region becomes larger simultaneous with process development.

Discrete changes in cytoplasmic organization were associated with the transition from epithelial to stellate morphology. An open delicate network of fine fibrils appears to become condensed, irregular, and thickened. There are a number of indications that these differences reflect changes in biological regulation and not preparation artifacts. (*a*) Regions of condensed cytoplasm were observed almost exclusively in (−)-isoproterenol-treated cells and not controls, even though treated and control cells were dehydrated and critical point dried during the same run. In very rare occurrences, condensed cytoplasm was observed in control cells, but only at the periphery in regions that appeared to be undergoing shape change as indicated by large projections and filopodia. (*b*) Condensed cytoplasm was observed almost exclusively in regions of embrasure development and in or near processes resulting from cytoplasmic withdrawal. (*c*) Transitions from one state of cytoplasmic organization to another occurred at clearly defined and sharp interfaces within cells, suggesting that the differences were not due to a solvent gradient formed during sample processing. (*d*) The presence of many delicate cytoplasmic structures including microspikes, thin and unsupported projections, and membrane lamellae suggest that specimen preparation was properly executed. The cytoplasmic changes indicate that different regions of the cytoplasm may undergo changes depending on their functions. Since intense study of the detailed structure of the cytoplasm has not yet produced a clear consensus (4, 5, 15, 26–28, 39), receptor-stimulated changes in cytoplasmic organization provide a unique opportunity to further investigate this fundamental problem.

The opinions and assertions contained herein are the private ones of the writers and are not to be construed as official or reflecting the views of the Department of Defense.

The work leading to this communication was supported in part by grants NS21219 and AA07155 (W. Shain), and by grant NS19676 (D. S. Forman). The HVEM was made available partly through Public Health Service grant PR1219 supporting the New York state high voltage electron microscope as a biotechnology resource.

Received for publication 14 December 1986, and in revised form 13 July 1986.

References

1. Allen, R. D., N. S. Allen, and J. L. Travis. 1981. Video-enhanced contrast, differential interference contrast (AVEC-DIC) microscopy: a new method capable of analyzing microtubule-related motility in the reticulopodial network of Allogromia laticollaris. *Cell Motil.* 1:291–302.

2. Awad, J. A., R. A. Johnson, K. H. Jakobs, and G. Schultz. 1983. Interactions of forskolin and adenylate cyclase. *J. Biol. Chem.* 258:2960–2965.
3. Bradford, M. M. 1976. A rapid and sensitive method for the quantitation of microgram quantities of protein utilizing the principle of protein-dye binding. *Anal. Biochem.* 72:248–254.
4. Bridgman, P. C., B. Kachar, and T. S. Reese. 1986. The structure of cytoplasm in directly frozen cultured cells. II. Cytoplasmic domains associated with organelle movements. *J. Cell Biol.* 102:1510–1521.
5. Bridgman, P. C., and T. S. Reese. 1984. The structure of cytoplasm in directly frozen cultured cells. I. Filamentous meshworks and the cytoplasmic ground substance. *J. Cell Biol.* 99:1655–1668.
6. Browning, E. T., C. O. Bromstrom, and V. E. Groppi, Jr. 1976. Altered adenosine cyclic 3′,5′-monophosphate synthesis and degradation by C-6 astrocytoma cells following prolonged exposure to norepinephrine. *Mol. Pharmacol.* 12:32–40.
7. Browning, E. T., and M. Ruina. 1984. Glial fibrillary acidic protein: Norepinephrine stimulated phosphorylation in intact C-6 glioma cells. *J. Neurochem.* 42:718–726.
8. Couchie, D., C. Fages, A. M. Bridoux, B. Rolland, M. Tardy, and J. Nunez. 1985. Microtubule-associated proteins and in vitro astrocyte differentiation. *J. Cell Biol.* 101:2095–2103.
9. Das, G. D. 1976. Differentiation of Bergmann glia in the cerebellum: a golgi study. *Brain Res.* 110:199–213.
10. deVillis, J., and G. Brooker. 1972. Effect of catecholamines on cultured glial cells: correlation between cAMP levels and lactic dehydrogenase induction. *Fed. Proc.* 31:513.
11. Dvorak, J. A., and W. F. Stotler. 1971. A controlled-environment culture system for high resolution light microscopy. *Exp. Cell Res.* 68:144–148.
12. Ebersolt, C., M. Perez, G. Vassent, and J. Bockaert. 1981. Characteristics of β_1- and β_2-adrenergic sensitive adenylate cyclases in glial cell primary cultures and their comparison with β_2-adrenergic sensitive adenylate cyclase of meningeal cell. *Brain Res.* 213:151–161.
13. Federoff, S., W. A. J. McAuley, J. D. Houle, and R. M. Devon. 1984. Astrocyte cell lineage. V. Similarity of astrocytes that form in the presence of dbcAMP in cultures to reactive astrocytes in vivo. *J. Neurosci. Res.* 12:15–27.
14. Haugen, A., and O. D. Laerum. 1978. Induced glial differentiation of fetal rat brain cells in culture: an ultrastructural study. *Brain Res.* 150: 225–238.
15. Heuser, J. E., and M. W. Kirschner. 1980. Filament organization revealed in platinum replicas of freeze-dried cytoskeletons. *J. Cell Biol.* 86: 212–234.
16. Lim, R., K. Mitsunobu, and W. K. P. Li. 1973. Maturation-stimulating effect of brain extract and dibutyryl cyclic AMP on dissociated embryonic brain cells in culture. *Exp. Cell Res.* 79:243–246.
17. Lin, L., C. F. Saller, and A. I. Salama. 1985. Rapid automated high-performance liquid chromatographic analysis of cyclic adenosine 3′-5′-monophosphate. Synthesis in brain tissues. *J. Chromatogr.* 341:43–51.
18. Madelian, V., D. L. Martin, R. Lepore, M. Perrone, and W. Shain. 1985. Beta-receptor stimulated and cAMP mediated taurine release from LRM55 glial cells. *J. Neurosci.* 5:3154–3162.
19. Madelian, V., and W. Shain. Regulation of isoproterenol-induced cAMP accumulation in LRM55 glial cells by phosphodiesterase. *J. Pharmacol. Exp. Ther.* In press.
20. McCarthy, K. D., J. Prime, T. Harmon, and R. Pollenz. 1985. Receptor-mediated phosphorylation of astroglial intermediate filament proteins in cultured astroglia. *J. Neurochem.* 44:723–730.
21. Narumi, S., H. K. Kimelberg, and R. S. Bourke. 1978. Effects of norepinephrine on the morphology and some enzyme activities of primary monolayer cultures from rat brain. *J. Neurochem.* 31:1479–1490.
22. Oey, J. 1975. Noradrenaline induces morphological alterations in nucleated and enucleated rat C-6 glioma cells. *Nature (Lond.).* 257:317–319.
23. Opler, L. A., and M. H. Makman. 1972. Mediation by cyclic AMP of hormone-stimulated glycogenolysis in cultured rat astrocytoma cells. *Biochem. Biophys. Res. Commun.* 46:1140–1145.
24. Pearlmutter, L. S., C. D. Tweedle, and G. I. Hatton. 1984. Neuronal/glial plasticity in the supraoptic dendritic zone: dendritic bundling and double synapse formation at parturition. *Neuroscience.* 13:769–779.
25. Pollenz, R. S., and K. D. McCarthy. 1986. Analysis of cyclic AMP-dependent changes in intermediate filament protein phosphorylation and cell morphology in cultured astroglia. *J. Neurochem.* 47:9–17.
26. Porter, K. R. 1984. The cytoplasmic matrix and the integration of cellular function. *J. Cell Biol.* 99:3s–238s.
27. Porter, K. R., and K. L. Anderson. 1984. The structure of the cytoplasmic matrix preserved by freeze-drying and freeze-substitution. *Eur. J. Cell Biol.* 29:83–96.
28. Ris, H. 1985. The cytoplasmic filament system in critical point-dried whole mounts and plastic-embedded sections. *J. Cell Biol.* 100:1474–1487.
29. Seamon, K., and J. W. Daly. 1981. Activation of adenylate cyclase by the diterpene forskolin does not require the guanine nucleotide regulatory protein. *J. Biol. Chem.* 256:9799–9801.
30. Shain, W. G., and D. L. Martin. 1984. Activation of β-adrenergic receptors stimulates taurine release from glial cells. *Cell. Mol. Neurobiol.* 4: 191–196.
31. Shain, W., V. Madelian, D. L. Martin, H. K. Kimelberg, M. Perrone, and R. Lepore. 1986. Activation of β-adrenergic receptors stimulates release of an inhibitory transmitter from astrocytes. *J. Neurochem.* 46:1298–1303.
32. Tardy, M., C. Fages, B. Rolland, A. Bardakdjian, and P. Gonnard. 1981. Effect of prostaglandins and dibutyryl cyclic AMP on the morphology of cells in primary astroglial cultures and on metabolic enzymes of GABA and glutamate metabolism. *Experientia (Basel).* 37:19–21.
33. Turner, J. N. 1981. Qualitative methods in stereo imaging. *Methods Cell Biol.* 22:1–363.
34. Turner, J. N., and A. J. Ratkowski. 1982. An improved double-tilt stage for the AEI-EM7 highvoltage electron microscope. *J. Microsc. (Oxf.).* 127:155–159.
35. Turner, J. N., W. G. Shain, V. Madelian, R. A. Grassucci, and D. S. Forman. 1986. High-voltage electron microscopy of astroglial cell whole mounts. *Proc. Annu. Meet. Electron Microsc. Soc. Am.*, 44th. 316–317.
36. Tweedle, C. D. 1983. Ultrastructural manifestations of increased hormone release in the neurohypophysis. *Prog. Brain Res.* 60:259–272.
37. Tweedle, C. D., and G. I. Hatton. 1984. Synapse formation and disappearance in adult rat supraoptic nucleus during different hydration states. *Brain Res.* 309:373–376.
38. Van Calker, D., M. Muller, and B. Hamprecht. 1978. Adrenergic- and β-receptors expressed by the same cell type in primary culture of perinatal mouse brain. *J. Neurochem.* 30:713–718.
39. Wolosewick, S. J., and K. R. Porter. 1979. Microtrabecular lattice of the cytoplasmic ground substance: artifact or reality? *J. Cell Biol.* 82: 114–139.